TOWARDS FIELD THEORY OF TURBULENCE

A PREPRINT

Alexander Migdal
Department of Physics, New York University
726 Broadway, New York NY 10003

December 22, 2024

ABSTRACT

We revisit the problem of stationary distribution of vorticity in three dimensional turbulence. Using Clebsch variables we construct an explicit invariant measure on stationary solutions of Euler equations with the extra condition of fixed energy flow/dissipation. The asymptotic solution for large circulation around large loops is studied as a WKB limit (instanton). The Clebsch fields are discontinuous across minimal surface bounded by the loop, with vorticity staying continuous and directed normal to the surface. This instanton is then compared with that from the Loop Equations. In addition to describing vorticity distribution over the minimal surface, this approach provides formula for the circulation PDF, which was elusive in the Loop Equations.

1 Introduction

Turbulence is well studied at a phenomenological level using numerical simulations of forced Navier-Stokes equations and fitting the data for distribution of various observables (such as moments of velocity and vorticity fields, as well as velocity circulation). The data suggest multi-fractal scaling laws implying some significant modifications of traditional Kolmogorov scaling by finite size vorticity structures with nontrivial distributions by shape, size and vorticity filling.

The microscopic theory, such as an effective Hamiltonian for the Gibbs distribution in ordinary critical phenomena, is missing. It is as though we already know the Newtonian dynamics but do not yet know the Boltzmann distribution. We can simulate the Navier-Stokes equations and average over time, but we lack basic definitions of stationary statistics for vorticity or velocity fields.

This statistics would be a fixed point of the evolution of the Hopf functional. If we knew such an analog of the Boltzmann law, we would be able to solve the theory analytically (at least in some extreme regime such as a large circulation limit for large loops). We would also have powerful Monte-Carlo methods with the Metropolis algorithm for fast simulation of this equilibrium statistics.

In this paper we are trying to fill this gap. We construct the distribution of vorticity and velocity in three dimensions which is manifestly conserved in Euler dynamics, while describing a steady energy cascade. It involves a two-component Clebsch field, as well as two auxiliary fields: one Bose field and one Majorana Grassmann field, both transforming as vectors in physical space R_3.

This theory represents a particular version of the Ising-Clebsch statistics of vorticity cells, suggested in our previous papers, but is much simpler to study, being a field theory in three dimensions.

In particular, the tails of the PDF for velocity circulation Γ over large fixed loops C are controlled by a classical field $\phi_a^{cl}(r)$ (instanton) concentrated around the minimal surface bounded by C.

The vorticity field is directed along the normal of this minimal surface, $\omega_\alpha(r) = \Omega(r) n_\alpha(r)$, with $\Omega(r)$ depending on local surface curvature (i.e. gradients of the $n(r)$). The resulting integral equation on a minimal surface was studied in the previous paper, where it was derived from the loop equations.

Here, we analyze these equations using Clebsch variables that map the loop C onto a loop $\gamma = \phi(C)$ in the complex plane. The circulation becomes the oriented area inside this (self-intersecting) loop. The minimal surface S_C bounded by C maps inside the curve $S_C \mapsto D : \partial D = \gamma$.

As for the scaling area law $\Gamma^2 \sim A_C$ that we derived in [1] from consistency of the loop equation, it now follows from simple power counting in the instanton equation.

2 Energy Flow as a Constraint to Vortex Statistics

As is well known, the energy is pumped into the turbulent flow from the largest scales (pipes, ships, etc.), and dissipated at the smallest scales due to viscosity effects. Let us see how that happens in some detail. Using Navier-Stokes equation

$$\dot{v_\alpha} = \nu\partial_\beta^2 v_\alpha - v_\beta\partial_\beta v_\alpha - \partial_\alpha p;\ \partial_\alpha v_\alpha = 0 \tag{1}$$

we have

$$\partial_t \int d^3r \frac{1}{2}v_\alpha^2 = \int d^3r\, \nu v_\alpha \partial_\beta^2 v_\alpha - v_\alpha\left(v_\beta\partial_\beta v_\alpha + \partial_\alpha p\right) = 0 \tag{2}$$

Compare the first term with $\int d^3r\omega_\alpha^2$:

$$\int d^3r\omega_\alpha^2 = \tag{3}$$

$$\int d^3r \tfrac{1}{2}(\partial_\alpha v_\beta - \partial_\beta v_\alpha)^2 = \tag{4}$$

$$\int d^3r(\partial_\alpha v_\beta)(\partial_\alpha v_\beta - \partial_\beta v_\alpha) = \tag{5}$$

$$-\int d^3r v_\alpha\partial_\beta^2 v_\alpha + \int d^3r\partial_\alpha\left(v_\beta(\partial_\alpha v_\beta - \partial_\beta v_\alpha)\right) \tag{6}$$

$$\tag{7}$$

So, we have the balance of two terms cancelling each other in the time derivative of energy : dissipation and pumping.

The mean energy dissipation rate (used in similar context in [2] as a constraint to Navier-Stokes equations) is

$$-\dot{E} = \nu\int_V d^3r\omega_\alpha(r)^2 \tag{8}$$

This is to be compared with the same energy flow from large scales:

$$-\dot{E} = \int_V d^3r v_\alpha\left(v_\beta\partial_\beta v_\alpha + \partial_\alpha p\right) + \nu\partial_\beta\left(v_\alpha(\partial_\beta v_\alpha - \partial_\alpha v_\beta)\right) \tag{9}$$

$$= \int_V d^3r\partial_\beta\left(v_\beta\left(p + \frac{1}{2}v_\alpha^2\right) + \nu v_\alpha(\partial_\beta v_\alpha - \partial_\alpha v_\beta)\right) \tag{10}$$

By the Stokes theorem, this reduces to the flow over the boundary ∂V of the integration box V:

$$-\dot{E} = \int_{\partial V} d\sigma_\beta\left(v_\beta\left(p + \frac{1}{2}v_\alpha^2\right) + \nu v_\alpha(\partial_\beta v_\alpha - \partial_\alpha v_\beta)\right) \tag{11}$$

Velocity is related to vorticity by the Biot-Savart law:

$$v_\alpha(r) = -e_{\alpha\beta\gamma}\partial_\beta\int d^3r'\frac{\omega_\gamma(r')}{4\pi|r-r'|} \tag{12}$$

In case there is no vorticity at the bounding sphere, the radial velocity would decrease as $1/|r|^3$ at infinity:

$$v_n(r) \to -\frac{r_\alpha}{4\pi|r|^4}Q_\alpha \tag{13}$$

$$Q_\alpha = e_{\alpha\beta\gamma}\int d^3r' r'_\beta\omega_\gamma(r') \tag{14}$$

In the case of an arbitrary bounding surface with the normal $n_\alpha(r)$, there would be the leading global vortex term:

$$v_n \propto \frac{n_\alpha(r)r_\beta}{|r|^3}\, e_{\alpha\beta\gamma}\int d^3r'\omega_\gamma(r') \tag{15}$$

which would cancel out provided the net integral of vorticity vanishes:

$$\int d^3r' \omega_\gamma(r') = 0 \tag{16}$$

The next term of multipole expansion of the Biot-Savart law will be the dipole:

$$v_n \propto \frac{n_\alpha}{|r|^3} e_{\alpha\beta\gamma} \int d^3r' r'_\beta \omega_\gamma(r') \tag{17}$$

which is the term we keep.[1] For a finite resulting flow after cancellation of powers of $|r|$, the pressure should behave as:

$$p(r) \to |r| g(n) \tag{18}$$

where n_α is the normal vector to the surface. This would correspond to finite force $\partial_\alpha p \sim 1$ which is distributed on a surface:

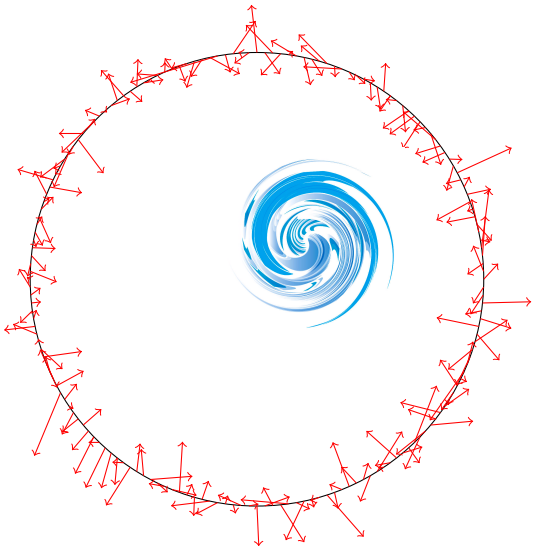

The resulting energy flux is:

$$-\dot{E} \to Q_\alpha f_\alpha \tag{19}$$

$$f_\alpha = \lim_{|V|\to\infty} \int_{r\in\partial V} \frac{d\sigma(r)}{4\pi|r|^3} n_\alpha(r) p(r) \tag{20}$$

This formula works for a generic bounding surface $S = \partial V$, in a limit when it is blown up to infinity. For a sphere, it becomes an average over unit vectors $n \in S_2$:

$$f_\alpha = \int_{n\in S_2} \frac{d^2n}{4\pi} n_\alpha g(n) = \langle n_\alpha g(n) \rangle_{n\in S_2} \tag{21}$$

This random force f_α would have some unknown PDF depending upon the specific microscopic mechanism of energy pumping:

$$dP(\vec{f}) = P(\vec{f}) d^3 f \tag{22}$$

The natural assumption is that this PDF is Gaussian, in accordance with the Central Limit Theorem for an average of large number of uncorrelated forces on a surface of a remote sphere.

[1] This geometry, with finite cell confining vorticity and energy flow being pumped from a distant boundary surface, was recently realized in beautiful experiments by [3], where the vortex rings were initially shot from the eight corners of a glass cubic tank, and a stable vorticity cell (a confined vorticity "blob" in their terms) was created and observed and studied in the center of the tank. The energy was pumped in pulses from eight corners and the vorticity distribution inside the cell was consistent with K41 scaling. Reynolds numbers in that experiment were not large enough for our instanton, but at least the energy flow entering from the boundary and dissipating in a vortex cell inside was implemented and studied in real water.

The asymptotic behavior of the normal component of velocity on a bounding sphere can be regarded as a Neumann boundary condition for solution of the Laplace equation $\nabla^2 v_\alpha = e_{\alpha\beta\gamma}\partial_\beta\omega_\gamma$. This behaviour is parameterized by the above vector Q in (13). Note that this vector is not invariant with respect to translation of coordinates. By specifying this vector we effectively are specifying the center of mass of the vorticity distribution inside, relative to the center of the volume inside bounding surface.

Note that while the dissipation formula (8) has the space integral supported on high vorticity regions, the incoming energy flow is concentrated on the bounding surface. The energy balance (2) requires that these two values of energy flow are equal. All the energy pumped from the boundary dissipates by viscosity at small scales inside vorticity cells. This provides the relation between vorticity distribution and the random force:

$$-\int_V d^3r\nu\omega_\alpha^2(r) + f_\alpha \int_V d^3r e_{\alpha\beta\gamma} r_\beta \omega_\gamma(r) = 0 \tag{23}$$

3 Statistical Mechanics

It is significant that this relation involves distribution of vorticity in the cell, where all dissipation is taking place. The second term comes from the flow through the boundary at infinity, but it involves the vorticity inside the cell. All the boundary conditions at infinity are represented by a (Gaussian) random vector force $\vec{f}$.

Note that this is **not** the same as postulating the energy spectrum of the pumping forces. We have only one vector with Gaussian distribution with some unknown variance.

In the following section, we are going to add this constraint not as a delta function in microcanonical distribution, but rather as exponential factor, inserted in canonical distribution with corresponding Lagrange multiplier λ. The motivation is the same as in statistical mechanics. We assume there is a "thermostat" interacting with a subsystem, with subsystem exchanging energy flow with "thermostat".

This is not the Gibbs distribution, of course, and the term "thermostat" does not mean that this chemical potential λ is related to the temperature.

Here is a physical picture we see as an origin of this thermodynamics. Consider a subsystem – single vorticity cell. The energy flowing through the infinite boundary is related to the net dipole moment in (14). This involves contributions from the other cells over the whole space, which act as a "thermostat".

The net energy flow constraint (23) tells us that net flow from the bounding surface is dissipated in all the cells, the subsystem as well as the thermostat. If we single out the dissipation inside the subsystem, then there is a missing piece, both the contribution of other cells to the net dipole moment (14) and the dissipation terms $\int_V d^3r\nu\omega_\alpha^2(r)$ inside these other cells.

Therefore, the equation (23) adds up from the subsystem and from the thermostat. If we single out the subsystem $\mathcal{E}$, there will be an extra fluctuating term $\mathcal{E}'$. The exponential distribution with Lagrange multiplier for the subsystem energy flow accounts for that extra term. The Lagrange multiplier comes about as logarithmic derivative of the phase space of the thermostat with respect to energy of the subsystem (in this case the energy flow).

Technically, we have (with $d\Gamma'$ representing the phase space element for the thermostat)

$$\int d\Gamma' \delta\left(\mathcal{E}' + \mathcal{E}\right) \propto \exp\left(S(-\mathcal{E})\right) \tag{24}$$

where $S(\mathcal{E})$ is an entropy (logarithm of total phase space volume of the hyper surface of energy flow constraints) of the thermostat. The statistical mechanics then proceeds with expanding this entropy in the (relatively small) contribution to the energy flow from the subsystem

$$S(-\mathcal{E}) \to S(0) - \lambda\mathcal{E} \tag{25}$$

$$\lambda = S'(0) \tag{26}$$

In case of microcanonical distribution, this entropy counted the volume of the energy hyper surface in phase space and we had $\lambda = \beta$.

In our case (see below) we are going to integrate over space of so called Generalized Beltrami Flows, so this entropy will count the volume of the hyper surface of energy flow constraint in the space of these flows. But the general philosophy of interaction between the thermostat and the subsystem via exchange of thermodynamic variables, fixed by certain fugacities (Lagrange multipliers for microscopic constraints) is the same here.

4 Generalized Beltrami Flow

Let us go deeper into the hydrodynamics.

We parameterize the vorticity by two-component Clebsch field $\phi = (\phi_1, \phi_2) \in R_2$:

$$\omega_\alpha = \frac{1}{2} e_{\alpha\beta\gamma} e_{ij} \partial_\beta \phi_i \partial_\gamma \phi_j \tag{27}$$

The Euler equations are then equivalent to passive convection of the Clebsch field by the velocity field:

$$\partial_t \phi_a = -v_\alpha \partial_\alpha \phi_a \tag{28}$$

$$v_\alpha(r) = \frac{1}{2} e_{ij} \left(\phi_i \partial_\alpha \phi_j\right)^\perp \tag{29}$$

Here $V^\perp$ denotes projection to the transverse direction in Fourier space, or:

$$V^\perp_\alpha(r) = V_\alpha(r) + \partial_\alpha \partial_\beta \int d^3 r' \frac{V_\beta(r')}{4\pi |r - r'|} \tag{30}$$

One may check that projection (29) is equivalent to the Biot-Savart law (12).

The conventional Euler equations for vorticity:

$$\partial_t \omega_\alpha = \omega_\beta \partial_\beta v_\alpha - v_\beta \partial_\beta \omega_\alpha \tag{31}$$

follow from these equations.

The Clebsch field maps R_3 to R_2 and the velocity circulation around the loop $C \in R_3$:

$$\Gamma(C) = \oint_C dr_\alpha v_\alpha = \oint_{\gamma_2} \phi_1 d\phi_2 = \text{Area}(\gamma_2) \tag{32}$$

becomes the oriented area inside the planar loop $\gamma_2 = \phi(C)$. We discuss this relation later when we build the Clebsch instanton.

The most important property of the Clebsch fields is that they represent a p, q pair in this generalized Hamiltonian dynamics. The phase-space volume element $D\phi = \prod_x d\phi_1(x) d\phi_2(x)$ is invariant with respect to time evolution, as required by the Liouville theorem. We will use it as a base of our distribution.

The generalized Beltrami flow (GBF) corresponding to stationary vorticity is described by $F_\alpha(x) = 0$ where:

$$F_\alpha \stackrel{\text{def}}{=} \omega_\beta \partial_\beta v_\alpha - v_\beta \partial_\beta \omega_\alpha \tag{33}$$

These three conditions are in fact degenerate, as $\partial_\alpha F_\alpha = 0$. So, there are only two independent conditions, the same number as the number of local Clebsch degrees of freedom. However, as we see below, relation between vorticity and Clebsch field is not invertible.

There is some gauge invariance (canonical transformation in terms of Hamiltonian system, or area preserving diffeomorphisms geometrically)[2].

$$\phi_a(r) \Rightarrow G_a(\phi(r)) \tag{34}$$

$$\det \frac{\partial G_a}{\partial \phi_b} = \frac{\partial(G_1, G_2)}{\partial(\phi_1, \phi_2)} = 1. \tag{35}$$

These transformations manifestly preserve vorticity and therefore velocity. [3]

[2] I am grateful to Pavel Wiegmann for drawing my attention to this invariance.

[3] These variables and their ambiquity were known for centuries [4] but they were not utilyzed within hydrodynamics until pineering work of Khalatnikov [5] and subsequent works of Kuznetzov and Mikhailov [6] and Levich [7] in early 80-ties. Modern mathematical formulation in terms of symplectomorphisms was initiated in [8]. Derivation of K41 spectrum in weak turbulence using kinetic equations in Clebsch variables was done by Yakhot and Zakharov [9].

In my work [10] the Clebsch variables were identified as major degrees of freedom in statistics of vortex cells and their potential relations to string theory was suggested. Finally, in recent work [11] I identified the surface degrees of freedom of the vortex cells as $U(1)$ compactified critical $c = 1$ string in two dimension, which was exactly solved by means of matrix models.

In terms of field theory, this is an exact gauge invariance, rather than the symmetry of observables, much like color gauge symmetry in QCD. This is why back in the early 90-ties I referred to Clebsch fields as "quarks of turbulence". To be more precise, they are both quarks and gauge fields at the same time.

It may be confusing that there is another gauge invariance in fluid dynamics, namely the **volume** preserving diffeomorphisms of Lagrange dynamics. Due to incompressibility, the volume element of the fluid, while moved by the velocity field, preserved its volume. However, these diffeomorphisme are not the symmetry of the Euler dynamics, unlike the **area** preserving diffeomorphisms of the Euler dynamics in Clebsch variables.

One could introduce gauge fixing, for example the one mapping some surface bounded by a loop C inside a disk with the same area in Clebsch plane. We study the instanton in this gauge for the case of a planar loop in a later section of this paper. This gauge condition is linear and therefore it does not require any extra Faddeev-Popov ghosts.

The global description of the orbits of these symplectomorphisms is a hard mathematical problem which we do not address here. This subject deserves professional mathematical investigation.

Note also that our condition comes from the Poisson bracket with Hamiltonian $H = \int d^3r \frac{1}{2} v_\alpha^2$

$$F_\alpha(r) = [\omega_\alpha, H] = \tag{36}$$

$$\int d^3r' \frac{\delta \omega_\alpha(r)}{\delta \phi_i(r')} e_{ij} \frac{\delta H}{\delta \phi_j(r')} = \tag{37}$$

$$- \int d^3r' \frac{\delta \omega_\alpha(r)}{\delta \phi_i(r')} v_\lambda(r') \partial_\lambda \phi_i(r') \tag{38}$$

We only demand that this integral vanish. The stationary solution for Clebsch would mean that the integrand vanishes locally, which is too strong. We could not find any finite stationary solution for Clebsch field even in the limit of large circulation over large loop.

So, the GBF does not correspond to stationary Clebsch field – there are dynamical gauge transformations $\partial_t \phi_a = -v_\alpha \partial_\alpha \phi_a + e_{ab} \frac{\partial h(\phi)}{\partial \phi_b}$ with some unknown function $h(\phi)$ in the equations of motion (28) .

5 Our Main Conjecture

We propose the following grand canonical ensemble:

$$dZ = dP(\vec{f}) D\phi \delta_{\mathrm{FP}} [F|\phi] \exp\left(-\lambda \left(\int_V d^3r \nu \omega_\alpha^2 - f_\alpha \int_V d^3r e_{\alpha\beta\gamma} r_\beta \omega_\gamma \right) \right) \tag{39}$$

where δ_{FP} is the Faddeev-Popov delta functional

$$\delta_{\mathrm{FP}}[F|\phi] = \det \frac{\delta F_\alpha}{\delta \phi_b} \int DU \exp\left(\imath \int d^3x U_a(x) F_a(x) \right) \tag{40}$$

The functional determinant $\det \frac{\delta F_\alpha}{\delta \phi_b}$ compensates for transformation of our constraint F with respect to evolution (31) making our measure conserved as required by the Liouville theorem.

We need to be more specific here. What is the determinant of the operator where the left index is vector and the right one is Clebsch index? The left index transforms as vector under $O(3)$ rotations while the right index transforms covariantly under symplectomorphisms?

The only definition we found which satisfies desired symmetry properties is the following one. Consider Poisson bracket

$$[F_\alpha(x), F_\beta(y)] = \int d^3z \frac{\delta F_\alpha(x)}{\delta \phi_a(z)} e_{ab} \frac{\delta F_\beta(y)}{\delta \phi_b(z)} \tag{41}$$

It is invariant with respect to symplectomorphisms as one can readily check.

$$e_{ab} \frac{\partial G_a}{\partial \phi_{a'}} \frac{\partial G_b}{\partial \phi_{b'}} = e_{a'b'} \det \frac{\partial G_a}{\partial \phi_b} = e_{a'b'} \tag{42}$$

From the point of view of matrix products in functional space this Poisson bracket is a product of three operators $\frac{\delta F}{\delta \phi} \times \hat{E} \times \frac{\delta F}{\delta \phi}^T$, where $\hat{E}_{a,b}(x,y) = e_{a,b} \delta(x-y)$. This makes determinant of Poisson bracket equal to the square of our determinant times $\det \hat{E} = 1$.

Henceforth our determinant can be defined as a pfaffian[4]

$$\det \frac{\delta F_\alpha}{\delta \phi_b} \equiv \sqrt{\det \left[F_\alpha(x), F_\beta(y)\right]} = \text{pf}\left(\left[F_\alpha(x), F_\beta(y)\right]\right) \tag{43}$$

There are zero modes associated with conservation

$$\frac{\partial}{\partial x_\alpha}\left[F_\alpha(x), F_\beta(y)\right]) = 0,\ \frac{\partial}{\partial y_\beta}\left[F_\alpha(x), F_\beta(y)\right] = 0 \tag{44}$$

So this determinant formally would be zero, unless we project out these zero modes. Otherwise it is well defined invariant kernel with well defined eigensystem.

The Lagrange multiplier λ is conjugate to the energy flow constraint, so we have to use the thermodynamic relation

$$\mathcal{E} = -\frac{\partial \log Z}{\partial \lambda} \tag{45}$$

where $\mathcal{E}$ is the energy flow from the "thermostat" to the subsystem under consideration.

Note that our distribution does not fix the scale of the Clebsch fields.

6 Finite Dimensional Examples

In a one dimensional rather than functional case, our distribution would be just the sum of delta functions of all the roots R of F:

$$\delta_{\text{FP}}[F|\phi] = \sum_{R:F[R]=0} \delta(\phi - R)\,\text{sign}\,F'(R) \tag{46}$$

$$\int D\phi \delta_{\text{FP}}[F|\phi]\mathcal{F}[\phi] = \sum_{R:F[R]=0} \mathcal{F}[R]\,\text{sign}\,F'(R) \tag{47}$$

The finite dimensional analog of GBF would be the roots of F which are time-independent. Even if the function itself evolves with time, the Faddeev-Popov delta function projects on these conserved roots with unit coefficients.

Let us study our distribution for a simple example of N dimensional particle moving in the potential well with Hamiltonian:

$$H(\vec{p}, \vec{q}) = \frac{\vec{p}^2}{2} + U(\vec{q}) \tag{48}$$

the steady state equations would be simply with $U_i = \partial_i U, U_{ij} = \partial_i \partial_j U$:

$$\phi = (p_i, q_i) \tag{49}$$

$$F_\alpha = (-U_i, p_i) \tag{50}$$

$$[F_\alpha, F_\beta] = \begin{pmatrix} 0, U_{i,j} \\ -U_{j,i}, 0 \end{pmatrix} \tag{51}$$

$$J = |\det U_{ij}| \tag{52}$$

Following our prescription in this case would lead to the distribution:

$$P(\vec{p}, \vec{q}) = \sum_{\vec{r}:\nabla U(r)=0} \delta(\vec{p})\delta(\vec{q} - \vec{r}) \tag{53}$$

which corresponds to a particle sitting at the local extrema r of the potential well with zero momentum. Even in this elementary example we see a complication. Consider axial symmetric potential of sombrero hat.

$$U = \frac{1}{2}\left(\vec{q}^2 - 1\right)^2 \tag{54}$$

There is a maximum at the origin and degenerate minimum: a sphere $\vec{q}^2 = 1$. We get determinant $\det U_{ij} \propto (-1)^N$ at the maximum, positive $\det U_{ij}$ at $N = 1$ and zero determinant at $N > 1$ at the minimum. The zero determinant at $N > 1$ comes because of the zero modes corresponding to rotations of this minimal sphere.

[4]We define pfaffian as a positive square root of determinant of anti-symmetric matrix.

This is clearly not what we need: to reject the maximum and keep the minimum. To reject the maximum we need to demand that the whole matrix of second derivatives is positive definite, not just its determinant.

To remove the fictitious zero weight, let us add a linear force, which will act as gauge fixing

$$U = \frac{1}{2}\left(\vec{q}^2 - 1\right)^2 - \vec{f}.\vec{q} \tag{55}$$

Now, at arbitrary f there will be only one stable minimum and we shall pick it, and we can tend $\vec{f} \to 0$.

7 Lyapunov Stability and Theta Factor

In general case, we have to fix the gauge[5] and eliminate all the unstable GBF.

This Lyapunov stability of GBF is in fact determined by another kernel

$$L_{\alpha\beta}(x,y) = \frac{\delta F_\alpha(x)}{\delta \omega_\beta(y)} \tag{56}$$

which is not symmetric. For stability of our flow we need its eigenvalues (Lyapunov exponents) to all have negative or zero real part. There should not be any eigenvalues in the right semi-plane.

There is a simple identity which allows to count for a matrix $\hat{L}$ the number of eigenvalues with positive real part (which we want to reject here)

$$N_+(\hat{L}) = \lim_{\epsilon\to 0^+} \int_{-\infty}^{\infty} \frac{dz}{2\pi} \exp\left(\imath\,\epsilon z\right) \mathrm{tr}\, \frac{1}{\hat{L} + \imath\, z} \tag{57}$$

In our case this number must be zero, so that we introduce extra factor

$$\Theta[\omega] = \theta\left(\frac{1}{2} - N_+(\hat{L})\right) \tag{58}$$

Note that this formula does not rely on quantization of $N_+(\hat{L})$ which may not be valid for operators in Hilbert space. Even if there is a continuous distribution of eigenvalues, this $N_+(\hat{L})$ will remain positive in case there are some eigenvalues distributed in the right semi-plane. For any distribution in the left semi-plane including imaginary axis this $N_+(\hat{L})$ would remain zero. For infinite number of eigenvalues in right semi-plane $N_+(\hat{L}) \to +\infty$ so that theta function still works.

If we introduce the extended operator $\hat{L}(z) = \hat{L} + \imath\, z$

$$\mathrm{tr}\, \frac{1}{\hat{L}(z)} = -\imath\, \partial_z \log\det \hat{L}(z) \tag{59}$$

$$N_+(\hat{L}) = -\lim_{\epsilon\to 0^+} \int_{-\infty}^{+\infty} \frac{dz}{2\pi\imath} \exp\left(\imath\,\epsilon z\right) \partial_z \log\det \hat{L}(z) = \tag{60}$$

$$\frac{1}{2\pi}\Delta_+(z) \arg\det \hat{L}(z) \tag{61}$$

Here $\Delta_+(z)\arg F(z)$ stands for the total phase acquired by $F(z)$ when z goes around the anti-clockwise loop in upper semi-plane surrounding zeroes of $F(z)$. In other words, it counts all eigenvalues of $\hat{L}$ in the right semi-plane.

So, we have stability selection factor

$$\Theta[\omega] = \theta\left(\pi - \Delta_+(z) \arg\det \hat{L}(z)\right) \tag{62}$$

Using Fourier Transform of theta function we finally find

$$\Theta[\omega] = \int_{-\infty}^{\infty} \frac{dy}{2\pi(\imath\, y + 1)} \exp\left(\imath\, y \left(\pi - \Delta_+(z) \arg\det \hat{L}(z)\right)\right) \tag{63}$$

Coming back to our distribution with prescription (63) we see that the distribution is uniformly covering stable generalized Beltrami flows, and therefore is conserved in Euler dynamics. The gauge invariance remains unbroken at

[5] Without gauge fixing our determinant will formally be zero due to the zero modes corresponding to gauge transformation.

this stage. We do not know the general prescription of unambigous gauge fixing, but in case of our instanton we can present a unique gauge condition (see below).

This is clearly not the Gibbs distribution (which would be undesirable). We are looking for an alternative fixed point of the PDF evolution which is capable of describing fixed energy flow instead of fixed energy.

As we shall see below, the GBF provides an adequately rich space of steady solutions that can incorporate energy flow.

The velocity circulation PDF is generated by the further constraint in (39):

$$P\left(\Gamma|C\right)=\int dP(\vec{f})\int D\phi\delta\left[F_{\alpha}\right]\mathrm{pf}\left(\left[F_{\alpha},F_{\beta}\right]\right)\Theta[\omega] \tag{64}$$

$$\delta\left(\Gamma-\oint_{\gamma_2}\phi_1 d\phi_2\right)\exp\left(-\lambda\left(\nu\int_V d^3r\,\omega_{\alpha}(r)^2-f_{\alpha}\int_V d^3r\,e_{\alpha\beta\gamma}r_{\beta}\omega_{\gamma}(r)\right)\right) \tag{65}$$

By construction, this $P\left(\Gamma|C\right)$ satisfies the Euler Loop equations, as they are equivalent to

$$\left\langle\exp\left(\imath\,\gamma\oint_C d\vec{r}\vec{v}\right)\oint_C d\vec{r}\vec{v}\times\vec{\omega}\right\rangle=0 \tag{66}$$

which reduces by the Stokes theorem to the flow of $\nabla\times v\times\omega$ through the surface bounded by C. This flow vanishes by virtue of steady equations of motion (31) for ω.

Moreover, the cancellation of the functional determinant between the delta function and Pfaffian means that our PDF reduces to the average over space of all stable GBF. To be more precise, we have constructed an invariant measure in this space.

8 Ghost Fields

With our modified Faddeev-Popov delta functional we can still use their ghost fields but to get Pfaffian we need one Grassmann field, not two:

$$\int D\phi\ \mathrm{pf}\left(\left[F_{\alpha},F_{\beta}\right]\right)\delta[F_{\alpha}]=\int D\phi DUD\Psi\exp\left(\imath\ \left\langle U_{\alpha}|F_{\alpha}\right\rangle+\left\langle\Psi_{\alpha}\left|\left[F_{\alpha},F_{\beta}\right]\right|\Psi_{\beta}\right\rangle\right) \tag{67}$$

with Ψ_{α} being Grassman field and $\left\langle A|B\right\rangle,\left\langle A|X|B\right\rangle$ stands for vector and matrix products in functional space.

One may verify the simple re-scaling of Clebsch field leaves the measure invariant except for the random force PDF. The fields transform according to their dimensions:

$$\phi_a\Rightarrow\lambda\phi_a \tag{68}$$

$$U_{\alpha}\Rightarrow\lambda^{-4}U_{\alpha} \tag{69}$$

$$\Psi_{\alpha}\Rightarrow\lambda^{-3}\Psi_{\alpha} \tag{70}$$

The scale factors of λ emerging in the measure $D\phi D\Psi DU$ will all cancel among themselves since our measure is dimensionless (the Grassmann variable measures transforms with inverse Jacobian). As for the phase counter $\Theta[\omega]$ it is obviously invariant as the scaling of operator $\hat{L}$ does not affect its phase.

The distribution for the random force will break this scale invariance. The same is true with respect to time reversal, which corresponds to the interchange of ϕ_1,ϕ_2. The distribution again does not change, but the random force will break this invariance, if its PDF is not even with respect to reflection $f\Rightarrow-f$.

This representation of invariant measure with ghost fields is suitable for the perturbative expansion in a background of a classical solution (instanton), which, as we shall see, dominates the distribution in the case of large circulation around a large loop.

9 Clebsch Confinement

Let us look more closely at our functional integral. By naive counting of degrees of freedom it is just a number, as we have two degrees of freedom at each point in space and two independent local constraints (31), so that the whole integral reduces to a sum over solutions of these constraints, just as it did in the case of a particle in a potential well.

It is unfortunately not so simple: there is in fact a functional degeneracy of these constraints. First, one could shift vorticity by velocity times the arbitrary local scalar field $\vec{\omega} \Rightarrow \vec{\omega} + \phi(r)\vec{v}$ as long as $v_\alpha \partial_\alpha \phi = 0$ (meaning this field does not change along the flow). Also, from $\nabla \times \vec{v} \times \vec{\omega} = 0$ we can have $\vec{v} \times \vec{\omega} = \nabla F$ with arbitrary $F(x)$.

Naturally, we implied the ambiguity of the primary constraints as functionals of velocity and vorticity. As you start solving these constraints you will find that $F(x) = \nabla \left(p + \frac{1}{2}\vec{v}^2\right)$. This does not change the fact that these constraints are degenerate, as they do not involve pressure $p(r)$ and are satisfied with arbitrary pressure.

As for the Clebsch field itself, it can be transformed by arbitrary local area-preserving diffeomorphism, as noted in the previous section.

There is, however, a limit where the functional integral reduces to a classical flow (instanton) up to the symplectomorphism. This is the limit of large circulation Γ over a large loop C.

Let us first describe a qualitative physical picture of our instanton. It is similar in spirit to the magnetic monopole in 3-dimensional gauge theories. In these theories the ground state has condensate of monopoles there which leads to a dual Meissner effect of pushing electromagnetic field from the vacuum, leading to collapse of this field in thin flux tubes between charges.

This was the origin of confinement in 3D gauge theories, but of course, literally the same mechanism is absent here. There is no gauge invariance associated with velocity playing the role of vector potential. There is no $U(1)$ symmetry and no associated charges, and hence no monopoles either.

Our gauge symmetry involves the Clebsch fields and our analogues of monopoles are singular sheets in physical space where our gauge potential ϕ_a become multi-valued. And our analog of confinement is confinement of Clebsches, and our analog of gluon field shrinking to minimal surfaces bounded by quark loops is the vorticity shrinking to minimal surface in case large circulation over large loop is present.

We expect confinement phenomenon here, except instead of magnetic monopoles we have found different singular solutions leading to condensation of vorticity (our analog of magnetic field).

Here is this picture of vorticity condensation.

Comparing our two constraints (energy dissipation and fixed circulation) we observe that to minimize dissipation in effective Hamiltonian $\lambda\nu \int d^3 r \omega_\alpha^2$ at fixed circulation we need the vorticity to be concentrated in a thin layer (of viscous thickness h) around the minimal surface $S_{\min}(C)$ with area A_C surrounded by C and directed along the normal n_α to this surface. There are, of course, other vorticity cells randomly distributed all over space, with their own energy dissipations. We are considering the energy dissipation per cell $\mathcal{E}_{\text{cell}}$, assuming this cell covers the minimal surface bounded by the loop C.

In that case:

$$\Gamma \sim |\vec{\omega}| A_C \tag{71}$$

$$\mathcal{E}_{\text{cell}} \sim \nu |\vec{\omega}|^2 h A_C \sim \frac{\Gamma^2 \nu h}{A_C} \tag{72}$$

$$\Gamma^2 \sim \frac{\mathcal{E}_{\text{cell}} A_C}{\nu h} \tag{73}$$

Thus, with fixed energy dissipation, we have $\Gamma^2 \propto A_C$ as derived from the loop equations.

10 Clebsch instanton

Let us study this instanton solution in more detail.

The basic clue is that the Clebsch field can be multi-valued without affecting uniqueness of the vorticity. An example was presented in [6]

$$\omega_\alpha = A e_{ijk} e_{\alpha\beta\gamma} S_i \partial_\beta S_j \partial_\gamma S_k; \; S_i^2 = 1 \tag{74}$$

It can be rewritten in terms of our Clebsch fields in polar coordinates $\theta \in (0, \pi), \varphi \in (0, 2\pi)$ for the unit vector $S = (\sin\theta\cos\phi, \sin\theta\sin\phi, \cos\theta)$:

$$\phi_1 = 2A\cos\theta; \tag{75}$$

$$\phi_2 = \varphi \pmod{2\pi} \tag{76}$$

The second variable ϕ_2 is multi-valued, but vorticity is finite and continuous everywhere. The helicity $\int d^3 r v_\alpha \omega_\alpha$ was ultimately related to winding number of that second Clebsch field [6].

This is not to say that helicity plays any role in our instanton. We used it just as example to explain the significance of multi-valued Clebsch field.

We found another case of multi-valued Clebsch fields which are relevant to large circulation asymptotic behavior.

Let us seek a solution for the Clebsch fields, with discontinuity across the minimal surface bounded by C. At each side $S_\pm$ of the surface the normal derivative of ϕ_i vanishes so that ϕ varies only in local tangent plane:

$$[n_i \partial_i \phi_a]_{S_\pm} = 0 \tag{77}$$

however the values of $\phi_a^\pm$ differ, so that the discontinuity

$$\Delta\phi_a(r) = \phi_a^+ - \phi_a^- \neq 0 \tag{78}$$

At the edge C of this surface the discontinuity must disappear so that there is a unique Clebsch field everywhere in R_3 excluding S. [7]

The tangent vorticity will vanish on both sides, so that vorticity would be directed at the oriented normal to the surface and will be continuous, as only values of Clebsch field are jumping, but not the tangent plane derivatives.

Such surface cut out in R_3 is shown here for the loop shaped as soccer gates, Fig.2 with some symbolic thickness to stress that this is a hole cut in space. This is actual minimal surface for this bounding loop.

With $\phi_a(\xi)$ depending only on local coordinates $\xi = (\xi_1, \xi_2)$ on the minimal surface $R_\alpha(\xi)$ we have:

$$\Gamma = \int_{S_{\min}(C)} d\sigma_\alpha(r)\omega_\alpha(r), \tag{79}$$

$$\omega_\alpha(r) = n_\alpha(r)\Omega(r) \tag{80}$$

$$\Omega(r) = \frac{1}{\sqrt{g}} \frac{\partial(\phi_1, \phi_2)}{\partial(\xi_1, \xi_2)} \tag{81}$$

where g is determinant of the induced metric $g_{ij} = \partial_i R_\alpha \partial_j R_\alpha; i, j = 1, 2$. Geometrically, this Ω is the ratio of area element in Clebsch plane to that on a minimal surface.

It is important though that this $\Omega(r)$ factor can be extended in linear vicinity of the surface. Namely, in the linear vicinity in the normal direction it does not depend upon the normal coordinate z as it follows from our condition (77) on normal derivatives of Clebsch field

$$n_\alpha \partial_\alpha \Omega(r) = 0 \tag{82}$$

11 Clebsch jumps across Minimal surface

Let us verify it. In linear vicinity of local tangent plane to the surface its equation reads (with K_1, K_2 being principal curvatures at this point)

$$z - \frac{K_1}{2}x^2 - \frac{K_2}{2}y^2 = 0 \tag{83}$$

$$n_i = \frac{(-K_1 x, -K_2 y, 1)}{\sqrt{1 + K_1^2 x^2 + K_2^2 y^2}} = (0, 0, 1) + O(x, y) \tag{84}$$

$$\Omega = n_\alpha \omega_\alpha \to \frac{1}{2} e_{ij} e_{ab} \partial_i \phi_a \partial_j \phi_b + O(x, y) \tag{85}$$

$$n_\alpha \partial_\alpha \Omega(r) \to e_{ij} e_{ab} \partial_i \partial_z \phi_a \partial_j \phi_b + O(x, y) \tag{86}$$

The mixed derivatives $\partial_i \partial_z \phi_a$ vanish at $x = y = z = 0$ for our boundary conditions.

Self-consistency of this solution for Clebsch parameterization requires that this surface should be a minimal surface.

[6] To be more precise, it was Hopf invariant on a sphere S_3 instead of real space R_3 (see [6] for details).

[7] We actually assume that the Clebsch field goes to zero off the surface so that vorticity stays finite in narrow layer around minimal surface. The thickness of determined by viscosity effects which we do not consider here (see discussion below).

Indeed, let us assume that ϕ_a has a discontinuity along some surface, with normal derivatives vanishing on both sides of the cut in R_3. In this case we would have vorticity proportional as the normal n_α to that surface with coefficient $\Omega(r)$ depending only on the local tangent coordinates, no z dependence in linear vicinity.

The vorticity conservation $\partial_\alpha \omega_\alpha = 0$ would then lead to the equation

$$0 = \partial_\alpha \omega_\alpha = \partial_\alpha \left(n_\alpha \Omega \right) = \Omega \partial_\alpha n_\alpha + n_\alpha \partial_\alpha \Omega \tag{87}$$

The term $\partial_\alpha n_\alpha$ here involves the surface derivatives as in $n_\alpha \partial_\beta n_\alpha = \frac{1}{2}\partial_\beta n^2 = 0$. Therefore

$$\partial_\alpha n_\alpha = \left(\delta_{\alpha\beta} - n_\alpha n_\beta \right) \partial_\beta n_\alpha = -K_1 - K_2 \tag{88}$$

which is the divergence in the tangent plane, or trace of external curvature tensor (see [1] for detailed discussion).

We see, that in general, this trace of external curvature tensor of the surface is equal to logarithmic derivative of Ω in normal direction

$$K_1 + K_2 = n_\alpha \partial_\alpha \log \Omega \tag{89}$$

In particular, for our boundary condition, with vanishing normal derivatives of Clebsch field and therefore vorticity, we arrive at the Plateau equation for the minimal surface $K_1 + K_2 = 0$.

Conversly, for arbitrary surface we would have to modify the boundary condition to satisfy this relation. Namely, we would have mixed boundary conditions

$$\left[\partial_z \phi_a \right]_{S_\pm} = A \left[\phi_a \right]_{S_\pm} \tag{90}$$

with local scalar A being mean external curvature

$$A = \frac{K_1 + K_2}{2} \tag{91}$$

This is quite remarkable: Clebsch field is allowed to have jumps across minimal surface as long as its normal derivatives vanish at each side of this surface!

12 Master Equation

Let us stress that vorticity is finite: the tangent components vanish because of vanishing normal derivatives of Clebsch field and normal components are determined by tangent derivatives of Clebsch field which are finite.

This discontinuity of the Clebsch field is compatible with vorticity being single valued like it was in case of helical flow. Note that gradients of vorticity are also finite. The tangent gradients are finite because the Clebsch field is assumed to be differentiable in tangent plane. The normal derivatives simply vanish as they are related to tangent derivatives of normal derivatives of Clebsch fields.

The viscous effects, generated by the term $\nu \partial_\beta^2 \omega_\alpha$ in vorticity evolution equation, would blow up, indeed. Therefore, the slot in space would in fact become a pancake with viscous thickness h surrounding the minimal surface. The gradients of vorticity would be smoothed by viscous dissipation effects in this region.

The resulting circulation is single-valued as well as vorticity, and it reduces to:

$$\Gamma^{\text{cl}}(C) = \int_{S_{\min}(C)} d\sigma(r) \Omega(r) = \int_{S_{\min}(C)} d\phi_1 \wedge d\phi_2 = \oint_C \phi_1 d\phi_2 \tag{92}$$

The constraint (33) reduces to the surface curl of $\vec{\omega} \times \vec{v}$, which is exactly the same integral equation for Ω as we derived from the Loop Equation in the WKB limit:

$$e_{pqi} n_p(r) \partial_q \left[\Omega(r) n_k(r) \left(\partial_i \delta_{kc} - \delta_{ic} \partial_k \right) \int_{S_{\min}(C)} d\sigma(r') \frac{\Omega(r') n_c(r')}{4\pi |\vec{r}' - \vec{r}|} \right] = 0 \tag{93}$$

This equation (we now call it the master equation) was analyzed in detail and solved numerically by *Mathematica*® code in [1]. This code builds the minimal triangulated surface for arbitrary external loop C and then solves this integral equation on this surface by multidimensional minimization, with the unknown variables being the values of Ω associated with elementary triangles of the surface.

This can be done with high precision for hundreds of thousands of triangles, which is sufficient to reach the continuum limit. On a supercomputer, one could continue to millions of triangles if needed. As compared to the initial Navier-Stokes problem, this is a reduction of the $3+1$ dimensional unstable problem to the 2 dimensional stable one. Short of an explicit analytical solution, this is the best we could expect.

There are some boundary conditions at the boundary C of this minimal surface, where viscosity could not be neglected. These issues were analyzed in detail in that paper.

13 Circulation PDF

All these equations were homogeneous: they did not normalize Ω. As we see now, there is an effective Hamiltonian

$$H_{eff} = \lambda \int_{x \in S_{\min}} d\sigma(x)\Omega(x) \left(\nu\Omega(x) - f_\alpha e_{\alpha\beta\gamma} x_\beta n_\gamma(x)\right) \tag{94}$$

This Hamiltonian should be used to relate normalization of $\Omega(x)$ to the external random force f which provides the energy flow. Let us now introduce an area-normalized solution Ω_0, such that:

$$\Omega(x) = Z\Omega_0(x) \tag{95}$$

$$\int_{x \in S_{\min}} d\sigma(x)\Omega_0(x) = A_C \tag{96}$$

$$A_C = \int_{x \in S_{\min}} d\sigma(x) \tag{97}$$

We find quadratic dependence of effective Hamiltonian of Z

$$H_{eff} = \lambda \left(\nu Z^2 \int_{x \in S_{\min}} d\sigma(x)\Omega_0(x)^2 - Z f_\alpha \int_{x \in S_{\min}} d\sigma(x) e_{\alpha\beta\gamma} x_\beta n_\gamma(x) \right) \tag{98}$$

Minimizing over Z we find the following:

$$Z = \bar{M}_\alpha f_\alpha \tag{99}$$

$$\bar{M}_\alpha = \frac{\int_{x \in S_{\min}} d\sigma(x)\Omega_0(x) e_{\alpha\beta\gamma} x_\beta n_\gamma(x)}{2\nu \int_{x \in S_{\min}} d\sigma(x)\Omega_0(x)^2} \tag{100}$$

Here we recall that coordinate x_β here is counted from the center of the bounding sphere used to define energy flow. This vector is part of our boundary conditions and it depends on the random force f (see the next section).

We obtain average energy flow with arbitrary force:

$$\partial_t E_{\text{cell}} = -\nu A_C \bar{\Omega_0^2} \int dP(\vec{f}) \left(\bar{M}_\alpha f_\alpha\right)^2 \tag{101}$$

$$\bar{\Omega_0^2} = \frac{\int_{x \in S_{\min}} d\sigma(x)\Omega_0(x)^2}{A_C} \tag{102}$$

We observe that at fixed average energy flow, the vector $\bar{M}_\alpha$ scales as $\frac{1}{\sqrt{A_C}}$ and therefore:

$$\Gamma_C(f) = A_C \bar{M}_\alpha f_\alpha \sim \sqrt{A_C} \tag{103}$$

The distribution of circulation will now follow from the distribution for f:

$$P(\Gamma|C) = \int dP(\vec{f}) \delta\left(\Gamma - \Gamma_C(f)\right) \tag{104}$$

Note that the normalization factor $\bar{\Omega_0^2}$ explicitly depends on external curvature of the minimal surface, leading to deviations from naive area rule for curved loops.

14 Gaussian Forces and Wilson Loop

Now, let us recall that the random force f_α adds up from the large number of uncorrelated small forces on the surface of remote sphere in our boundary conditions. As such, it would be a Gaussian random variable with symmetric isotropic distribution

$$P(\vec{f}) \propto \exp\left(-\frac{1}{2}\frac{f_\alpha^2}{\sigma}\right) \tag{105}$$

As for the mean dipole moment $\bar{M}_\alpha$ it would be zero in absence of the random forcing, due to translation invariance. Random forcing breaks this invariance end freezes the center of mass of the vorticity cell, which results in finite $\bar{M}_\alpha$.

Our GBF distribution for the specific cell is translation invariant with respect to velocity and vorticity coordinates as well as the loop C translation by any constant vector $\vec{r} \Rightarrow \vec{r} + \vec{a}$ but that translation would shift the vector $\vec{Q}^{cell} = \int_{cell} d^3r \vec{r} \times \vec{\omega}$ by a vector $\vec{a} \times \int_{cell} d^3r \vec{\omega}(r)$.

True translation invariance would require shifting positions of ALL vortex cells by the same vector, not just the subsystem under consideration. Demanding that invariance relates our $\vec{Q}$ to the net sum of all $\vec{Q}$ for other cells of the thermostat.

That introduces some dependence of $\vec{Q}$ and hence $\vec{M}$ of the random force. You may write the relation like this

$$Q_\alpha^{cell}(\vec{f}) + \sum_{cell' \in Thermostat} Q_\alpha^{cell'}(\vec{f}) = 0 \tag{106}$$

This relation holds at fixed force which places each center of vorticity cell depending of $\vec{f}$ and that fixes each of dipole moments $Q_\alpha^{cell'}(\vec{f})$. Now, this relation is translation invariant provided net vorticity vanishes

$$\int_{cell} d^3r\vec{\omega} + \sum_{cell' \in Thermostat} \int_{cell'} d^3r\vec{\omega} = 0 \tag{107}$$

which is implied in our boundary conditions (we adjust pressure on the bounding surface so that we do not rotate fluid as whole). Coming back to the relation for a Q vector for subsystem

$$Q_\alpha^{cell}(\vec{f}) = -\sum_{cell' \in Thermostat} Q_\alpha^{cell'}(\vec{f}) \tag{108}$$

With small force compared to the vorticity scales, one would expand (the zero order term vanishes by space symmetry):

$$Q_\alpha^{cell}(\vec{f}) \to Q_{\alpha\beta} f_\beta + O(f^2) \tag{109}$$

In case of the surface cell we are considering this implies linear law

$$\bar{M}_\alpha = \frac{1}{\sqrt{A_C}} \mu_{\alpha\beta} f_\beta + O(f^2) \tag{110}$$

with some susceptibility tensor $\mu_{\alpha\beta}$ depending of the shape of vortex cell (the minimal surface in our limit). The factor $\frac{1}{\sqrt{A_C}}$ was introduced for correct normalization of the energy flow below.

Note that these leading linear terms preserve the time reversal symmetry (reflection of f), whereas the next, quadratic terms would already break this symmetry. The symmetry breaking effects as we shall see below, display themselves only for small circulations, and disappear in the tails of circulation PDF we are now studying.

In this case the PDF can be computed in explicit form. We have for the circulation

$$\Gamma_C = \sqrt{A_C} \mu_{\alpha\beta} f_\alpha f_\beta + O(f^3) \tag{111}$$

with μ related to the energy flow to the cell from the thermostat

$$\left\langle \partial_t E_{\text{cell}} \right\rangle \approx -\nu \bar{\Omega}_0^2 \sigma^2 \left((\text{tr}\,\mu)^2 + 2\text{tr}\,\mu^2 \right) \tag{112}$$

Apparently, at fixed mean energy flow there at least two solutions for susceptibility tensor $\mu = \pm\bar{\mu}$, with opposite signs, corresponding to positive and negative PDF tails:

$$\Gamma_C = \pm\sqrt{A_C} \bar{\mu}_{\alpha\beta} f_\alpha f_\beta \tag{113}$$

Note that only symmetric part of susceptibility tensor enters this relation for the circulation.

The Gaussian integral can be computed exactly for the generating function (our Wilson loop)

$$W(\gamma, C) = \left\langle \exp\left(\imath\,\gamma \frac{\Gamma_C}{\sqrt{A_C}}\right)\right\rangle = \frac{1}{2}\left(\frac{1}{\sqrt{\prod_{i=1}^{3}(1-2\imath\,\sigma\gamma\bar{\mu}_i)}} + \frac{1}{\sqrt{\prod_{i=1}^{3}(1+2\imath\,\sigma\gamma\bar{\mu}_i)}}\right) \tag{114}$$

where $\bar{\mu}_i$ are three real positive eigenvalues of symmetric tensor μ.

In general case these eigenvalues are all different. The Fourier integral

$$P(\Gamma|C) = \int_{-\infty}^{+\infty} \frac{d\gamma}{2\pi\sqrt{A_C}} \exp\left(-\imath\,\gamma\frac{\Gamma}{\sqrt{A_C}}\right) W(\gamma, C) \tag{115}$$

would be dominated by the nearest square root singularity in proper semi-plane depending of the sign of Γ

$$P(\Gamma|C) \to \frac{\text{const}}{\sqrt{|\Gamma|}} \exp\left(-\frac{|\Gamma|}{2\bar{\mu}_1\sigma\sqrt{A_C}}\right) \tag{116}$$

corresponding to the largest eigenvalue $\bar{\mu}_1$.

15 Flat Loop

In case of flat loop there is extra symmetry which allows us to go further, with a slightly different result. Namely, in this case the minimal surface is a flat disk inside this loop, and so the tensor $\mu_{\alpha\beta}$ is orthogonal to n_α

$$n_\alpha \bar{\mu}_{\alpha\beta} = 0 \tag{117}$$

where n_α is the normal to this plane. This makes one of the eigenvalues vanish.

$$\mu_3 = 0 \tag{118}$$

In that case the Fourier integral can be reduced to Bessel function of imaginary argument. In proper normalization ($P(0|C) = 1$)

$$P(\Gamma|C) = \exp\left(-\frac{1}{2}(a_1+a_2)|\Gamma|\right) I_0\left(\frac{1}{2}(a_1-a_2)\Gamma\right) \tag{119}$$

$$a_i = \frac{1}{2\bar{\mu}_i\sigma\sqrt{A_C}} \tag{120}$$

Asymptotically, at large $|\Gamma|(a_2 - a_1)$ we have

$$P(\Gamma|C) \to \frac{\exp\left(-a_1|\Gamma|\right)}{\sqrt{\pi(a_2-a_1)|\Gamma|}} \tag{121}$$

In symmetric case $a_2 = a_1$ we have $I_0(0) = 1$ and the spectrum is purely exponential. This is relevant to the square contour. In case when there is almost perfect symmetry in xy plane so that $a_2 - a_1 \ll a_1$ there is an intermediate regime when pre-exponential factor is far from constant (see Fig.1).

Let us now study the property of the Clebsch field for the flat case.

As described in my previous papers, in the case of a flat loop there is a trivial, constant solution for Ω in (81). This is because for a flat loop and flat surface the Biot-Savart integral for velocity will reduce to a gradient so that its curl will vanish. That solution was singular near the boundary, due to the growing viscous effect. It was argued in [1] that exactly at the boundary the Ω must oscillate so that the integral $\oint_C |dr|\Omega(r) = 0$.

So, we shall consider the arbitrary profile $\Omega(r)$ and analyze the corresponding Clebsch field. As is typical with instantons, the internal space is mapped into physical space.

Let us use the polar coordinates in x_1, x_2 plane : $x_1 + \imath\, x_2 = \rho e^{\imath\,\theta}$ and look for the similar representation of the Clebsch field:[8]

$$\phi_1 = f(\rho, \theta);\ \phi_2 = \theta \tag{122}$$

[8]This is gauge fixing from the point of view of our area-preserving diffeomorphisms. In general gauge the bounding curve in ϕ plane would become an arbitrary curve with the same area (= circulation). The angular variable on this curve will still match the one in physical space. The gauge fixing is equivalent to the choice of coordinates describing the Clebsch loop: polar, stereographic, Cartesian or whatever conformal map we may invent.

Then, using the metric $\sqrt{g} = \rho$ we find the simple equation:

$$\frac{1}{\rho}\frac{\partial f}{\partial \rho} = \Omega(\rho, \theta) \tag{123}$$

with solution

$$f(\rho, \theta) = \int_0^\rho d\rho' \rho' \Omega(\rho', \theta) \tag{124}$$

As long as $\Omega(\rho', \theta)$ is constant (which is not too close to the boundary), we have ϕ_1 grow as ρ^2. In the boundary layer Ω changes sign depending on the angular variable. Therefore, for some directions $f(\rho, \theta)$ will keep growing, while for others it will reach the peak and start decreasing.

16 Comparison with Numerical Experiments

The first large-scale simulations of circulation PDF [12] showed nearly exponential decay on both sides, with different slopes. As for the dependence upon the shape and area of the loop, they observed the area law as well as the deviations from the K41 scaling $\Gamma \sim A_C^{\frac{2}{3}}$. The moments $M_p(C) = \langle |\Gamma_C|^p \rangle$ were measured in an inertial range of sizes of the loop C. The results were interpreted as bi-fractal by these authors, in the sense that the K41 scaling law was transitioning to another with a lower scaling index $\alpha < \frac{2}{3}$.

The area law (for the flat loop) implies that the dimensionless ratios of these moments (as well as the PDF tails in proper normalization of the slope) to, for instance, $M_p^{\frac{1}{p}}, p \gg 1$, should not depend on the ratios of perimeter to the square root of area. As for the lower moments themselves, they show the clear dependence of this ratio. In particular, for the second moment this dependence is calculable [9]. We wrote *Mathematica*®code computing the second moment as a function of this ratio.

For higher moments, this dependence of the rectangle's aspect ratio should disappear up to the finite size corrections $C(p)P/A$, where P is a perimeter and A is the area inside, and $C(p)$ is some coefficient depending of p. The DNS data (Kartik Iyer, private communication) agree with these predictions.

The dependence of the dimensionless combinations of logarithms of moments $\frac{1}{p}\log M_p - \frac{1}{p-1}\log M_{p-1}$ of the aspect ratios of rectangular loop is strong enough for small p but seems to disappear at larger $p > 10$ (Kartik Iyer, private communication). This supports the universality of area law for flat loops.

The closer examination in collaboration with Kartik Iyer of the previous measurements [12] reveals the following picture. The effective scaling index $2\alpha_{eff}(p) = \frac{2}{p}\frac{\partial \log M_p(c)}{\partial \log A_C}$ starts at roughly 1.38 at p=0, passes through the K41 value $\frac{4}{3} = 1.33$ at $p = 3$ and then drops to 1.2 at $p = 10$. However, if one fits the whole curve after $p = 2$ it is evidently compatible with an asymptotic value of $2\alpha_{eff}(\infty) = 1$, corresponding to our prediction $\alpha = \frac{1}{2}$. See Fig.3

The reason lower moments are closer to K41 than higher moments is that lower moments are dominated by the tip of the PDF, whereas higher ones are dominated by the tails. The minimal surface instanton applies only to the high moments $M_p(C), p \to \infty$.

So there is no contradiction between the scaling observed in DNS and the asymptotic area law with scaling index $\alpha = \frac{1}{2}$.

The exponential law we derived at the end of the previous section perfectly matches the DNS data for flat rectangular loop from [12], as we analyzed that data together with Kartik Iyer. Fig.4.

At low Γ the breaking of time reversal is manifest because of the third moment, related to triple correlator of velocity field. However, at large Γ with proper normalization of the left tail, the PDF become perfectly linear and symmetric.

The apparent stretching of the exponential [12] is now understood as combination of a small Γ effect and low statistics at the high end of the spectrum $|\Gamma| > 20000\nu$, PDF $< 10^{-10}$, which should be excluded from the fit.

17 Connection to the String-Ising Model

In the previous paper [11] we outlined a geometric approach to Turbulence, with collections of vorticity cells of arbitrary shapes and sizes. The statistics of these cells was argued to be similar to that of the $\sigma = 1$ domains in the 3D Ising model in the magnetic field.

[9] Victor Yakhot and Sasha Polyakov, private communication

The surface degrees of freedom of these cells were found to be related to those of the Clebsch field and we argued that the effective Hamiltonian for these surface degrees of freedom was equivalent to the S^1 compactified critical string theory.

As for the bulk degrees of freedom coming from the Clebsch fields inside the cells, we have left that problem unsolved. We could not find the local effective Hamiltonian inside the cell which would be conserved and also invariant with respect to volume-preserving diffeomorphisms.

As we now understand it, the bulk PDF for the variables inside the vorticity cell is (64), with boundary condition $\phi_1^2 + \phi_2^2 = \text{const}$ on the surface of the cell. This is up to symplectic (gauge) transformations of the Clebsch field.

In a different gauge this circle in ϕ plane would become another closed curve γ with the same area. However, this is of no significance, since the relevant surface degree of freedom would still be an angular variable at this curve.

So we find no need for breaking of gauge symmetry at the bounding surface: gauge symmetry remains and simply redefines the curve in ϕ plane with the same angular variable.

The effective Hamiltonian for these surface degrees of freedom would follow from the effective Hamiltonian for the dissipation constraint:

$$H_d(D) = \int_D d^3 r \omega_\alpha^2 \tag{125}$$

which can be added with Lagrange multiplier λ to the effective Hamiltonian to fix the dissipation. Note that this involves vorticity, which is gauge invariant, so the choice of the curve γ above is irrelevant.

Therefore, we may leave it as a circle without losing generality.

The new partition function for the cell D is:

$$Z(\lambda|D) = \int dZ \exp\left(-\lambda H_d(D)\right) \tag{126}$$

with the condition on the Lagrange multiplier λ:

$$-\nu \frac{\partial \log Z(\lambda|D)}{\partial \lambda} = \langle \nu H_d(D) \exp\left(-\lambda H_d(D)\right)\rangle = \mathcal{E} \tag{127}$$

Let us consider the thin layer $L(D)$ of D of viscous thickness r_0 near the bounding surface ∂D. Our boundary conditions require that in polar coordinates $\phi = (R\cos\theta, R\sin\theta)$, $R = \text{const}$ at the boundary, so that in this layer the normal components of vorticity vanish. The remaining longitudinal components of vorticity are related to normal derivatives of R times longitudinal derivatives of ϕ:

$$\omega_i \propto R n_\alpha \partial_\alpha R e_{ij} g^{jk} \partial_k \theta \tag{128}$$

As a result, the integral over this boundary layer is

$$\int_{L(D)} d^3 r \omega_\alpha^2 \propto \int_{\partial D} d^2\xi \sqrt{g} g^{ij} \partial_i \theta \partial_j \theta \tag{129}$$

which is precisely the effective Action of the S^1 compactified string. As we argued in [11] the remaining Liouville effective action coming from the conformal metric g_{ij} on the boundary of the cell makes it a $c = 1$ critical 2D string which was exactly solved by matrix models.

This, however, does not yet solve our problem because of remaining Clebsch degrees of freedom inside the vorticity cell and the remaining dynamics of the cell surface.

This bounding surface ∂D should not be confused with the minimal surface of the previous section. The minimal surface in fact corresponds to the inside of the vorticity cell, where vorticity is directed along the normal to this surface.

One could visualize the vortex cell relevant for the large circulation over the large contour as a pita bread with velocity lines running in circles in the middle (the onion rings of the pita) so that vorticity is directed at the normal. Directly at the surface of the cell the vortex lines slide along. As for velocity, its normal component is not restricted except for conservation of the net volume, which means the net velocity flow must cancel in equilibrium.

Remember, we are considering the generalized Beltrami flows, where vorticity and velocity need not be collinear. In fact, the vorticity is perpendicular to velocity inside the cell. The mean vorticity used in the circulation estimate in the previous sections, should be understood as mean over the thickness of our pita bread. It may be tangential exactly at the surface but its mean across the normal direction is directed at the normal to the minimal surface.

If we consider the vorticity flux corresponding to large fixed circulation, it can be computed using an arbitrary Stokes surface, but the mechanics will be very different for the minimal surface which passes through the middle of the filling of the pita bread and some other surface bounded by the same loop C but going away from the minimal surface in the middle.

In the computation with the flux through the minimal surface, vorticity is directed along its normal and has the magnitude $\omega \sim \frac{1}{\sqrt{A}}$ which results in $\Gamma \sim \sqrt{A}$ after integration over the surface area.

If we blow up the soap film into a big bubble with a hole at C, the vorticity is present only near the loop and is finite there so that the net flux is proportional to perimeter $|C| \sim \sqrt{A}$.

Therefore, the result is the same but the computation is quite different. The difference between the perimeter and the square root of the minimal area must be compensated for by the dependence of vorticity near the loop of the angular variable along the loop. This is what the Stokes theorem dictates.

18 Discussion

I am stopping here at the most interesting place of our story. There are still some unsolved mysteries and some unproven conjectures.

First, it appears straightforward (though tedious) to verify the condition (31) in isotropic turbulence in numerical simulations of forced Navier-Stokes equations.

Second, the distribution of vorticity itself in the presence of large velocity circulation around a large loop can be measured in these simulations. Does it concentrate in our pita bread around the minimal surface?

Third, what is the origin of the mean dipole moment $\bar{M}(f)$? It influences the circulation PDF but we currently have no idea how to compute it. We postulated that it linearly depends upon the Gaussian external force but we lack the computation of corresponding susceptibility tensor.

As for the relation of the present field theory model to the String-Ising model [11] this is quite intriguing at a conceptual level, but does not help in practical computations. The WKB expansion around the minimal surface instanton is the only tunnel with some light at its end.

19 Acknowledgements

I am grateful to Sasha Polyakov, Katepalli R. Sreenivasan and Victor Yakhot for useful discussions of the physics of Navier-Stokes dissipation and to Pavel Wiegmann for discussions of both the physics and mathematics of Beltrami flow. Discussions with Grisha Falkovitch, Eugene Levich and Yaron Oz helped me understand better the random Beltrami flow and other aspects of turbulence in Euler dynamics, including the evidence coming from direct numerical simulations. I am grateful to Kartik Iyer for useful discussions of numerical data and providing the results of new DNS prior to publication.

Discussions with Eugene Kuznetsov and Samson Shatashvilli after my informal Zoom seminar helped me arrive at the step function prescription for the Lyapunov stability in my theory. I am grateful to them for these discussions.

Numerous discussions with Nikita Nekrasov both inspired me and helped me understand mathematical structures involved in my theory, especially the topology of Clebsch field and meaning of its discontinuities. His input was unique and precious. I also appreciate his timely reminder about WW.

This work is supported by a Simons Foundation award ID 686282 at NYU.

References

[1] Alexander Migdal. Analytic and numerical study of navier-stokes loop equation in turbulence, 2019. URL https://arxiv.org/abs/1908.01422v1.

[2] E Novikov. A new approach to the problem of turbulence, based on the conditionally averaged navier-stokes equations. *Fluid Dynamics Research*, 12(2):107–126, aug 1993. doi: 10.1016/0169-5983(93)90108-m. URL https://doi.org/10.1016%2F0169-5983%2893%2990108-m.

[3] T. Matsuzawa and W. Irvine. Realization of confined turbulence through multiple vortex ring collisions. Talk at the Flatiron Conference "Universality Turbulence Across Vast Scales", 03/12/2019.

[4] H. Lamb. *Hydrodynamics*. Dover Books on Physics. Dover publications, 1945. ISBN 9780486602561. URL https://books.google.com/books?id=237xDg7T0RkC.

[5] I.M. Khalatnikov. The hydrodynamics of solutions of impurities in helium ii. *Zh. Eksp. Teor. Fiz*, 23:169, 1952.

[6] E.A. Kuznetsov and A.V. Mikhailov. On the topological meaning of canonical clebsch variables. *Physics Letters A*, 77(1):37 – 38, 1980. ISSN 0375-9601. doi: https://doi.org/10.1016/0375-9601(80)90627-1. URL http://www.sciencedirect.com/science/article/pii/0375960180906271.

[7] E Levich. The hamiltonian formulation of the euler equation and subsequent constraints on the properties of randomly stirred fluids. *Physics Letters A*, 86(3):165–168, 1981.

[8] Jerrold Marsden and Alan Weinstein. Coadjoint orbits, vortices, and clebsch variables for incompressible fluids. *Physica D: Nonlinear Phenomena*, 7(1):305 – 323, 1983. ISSN 0167-2789. doi: https://doi.org/10.1016/0167-2789(83)90134-3. URL http://www.sciencedirect.com/science/article/pii/0167278983901343.

[9] Victor Yakhot and Vladimir Zakharov. Hidden conservation laws in hydrodynamics; energy and dissipation rate fluctuation spectra in strong turbulence. *Physica D: Nonlinear Phenomena*, 64(4):379 – 394, 1993. ISSN 0167-2789. doi: https://doi.org/10.1016/0167-2789(93)90050-B. URL http://www.sciencedirect.com/science/article/pii/016727899390050B.

[10] A. A. Migdal. Turbulence as statistics of vortex cells. In V.P. Mineev, editor, *The First Landau Institute Summer School, 1993: Selected Proceedings*, ... @Landau Institute Summer School: Institut Teoretičeskoj Fiziki Imeni L.D. Landau, pages 178–204. Gordon and Breach, 1993. ISBN 9782884491389. URL https://arxiv.org/abs/hep-th/9306152v2.

[11] Alexander Migdal. Turbulence, string theory and ising model, 2019. URL https://arxiv.org/abs/1912.00276v3.

[12] Kartik P. Iyer, Katepalli R. Sreenivasan, and P. K. Yeung. Circulation in high reynolds number isotropic turbulence is a bifractal. *Phys. Rev. X*, 9:041006, Oct 2019. doi: 10.1103/PhysRevX.9.041006. URL https://link.aps.org/doi/10.1103/PhysRevX.9.041006.

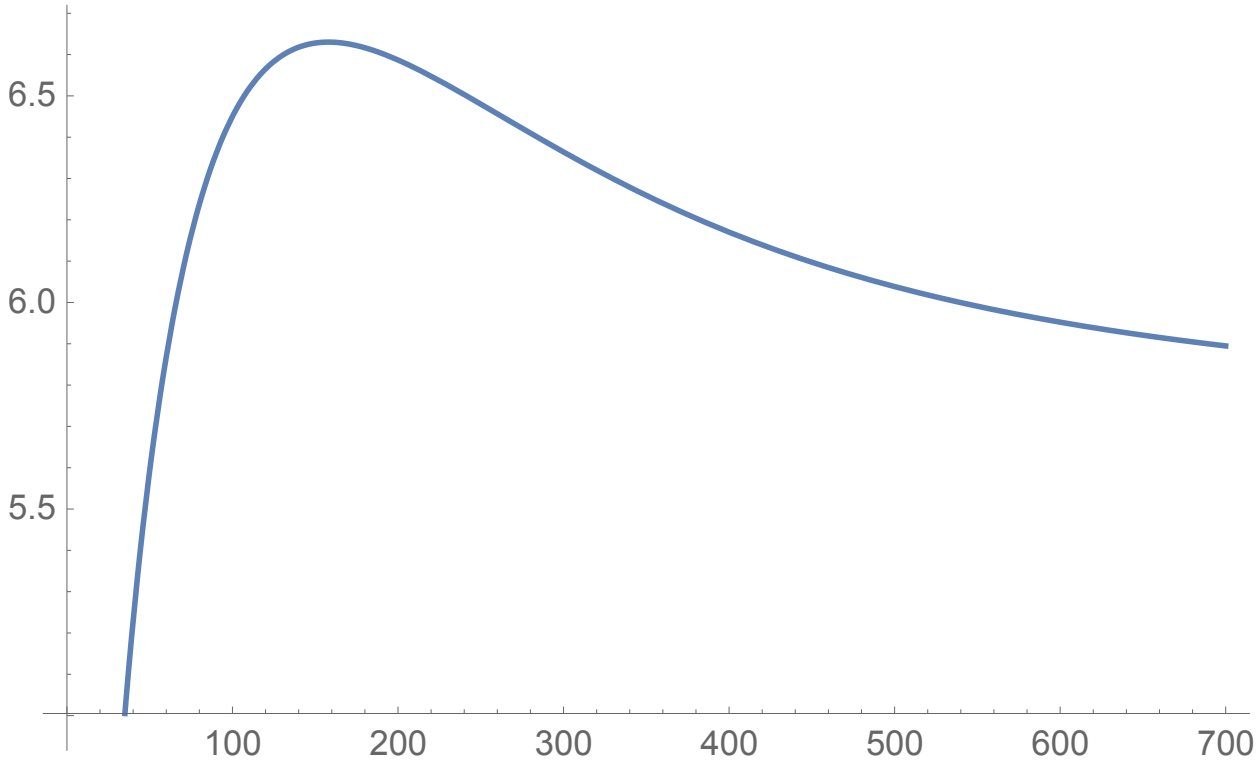

Figure 1: The pre-exponential factor $F(a_1\Gamma) = P(\Gamma|C)\exp(a_1\Gamma)\sqrt{a_1\Gamma}$ for $a_2 = 1.01a_1$

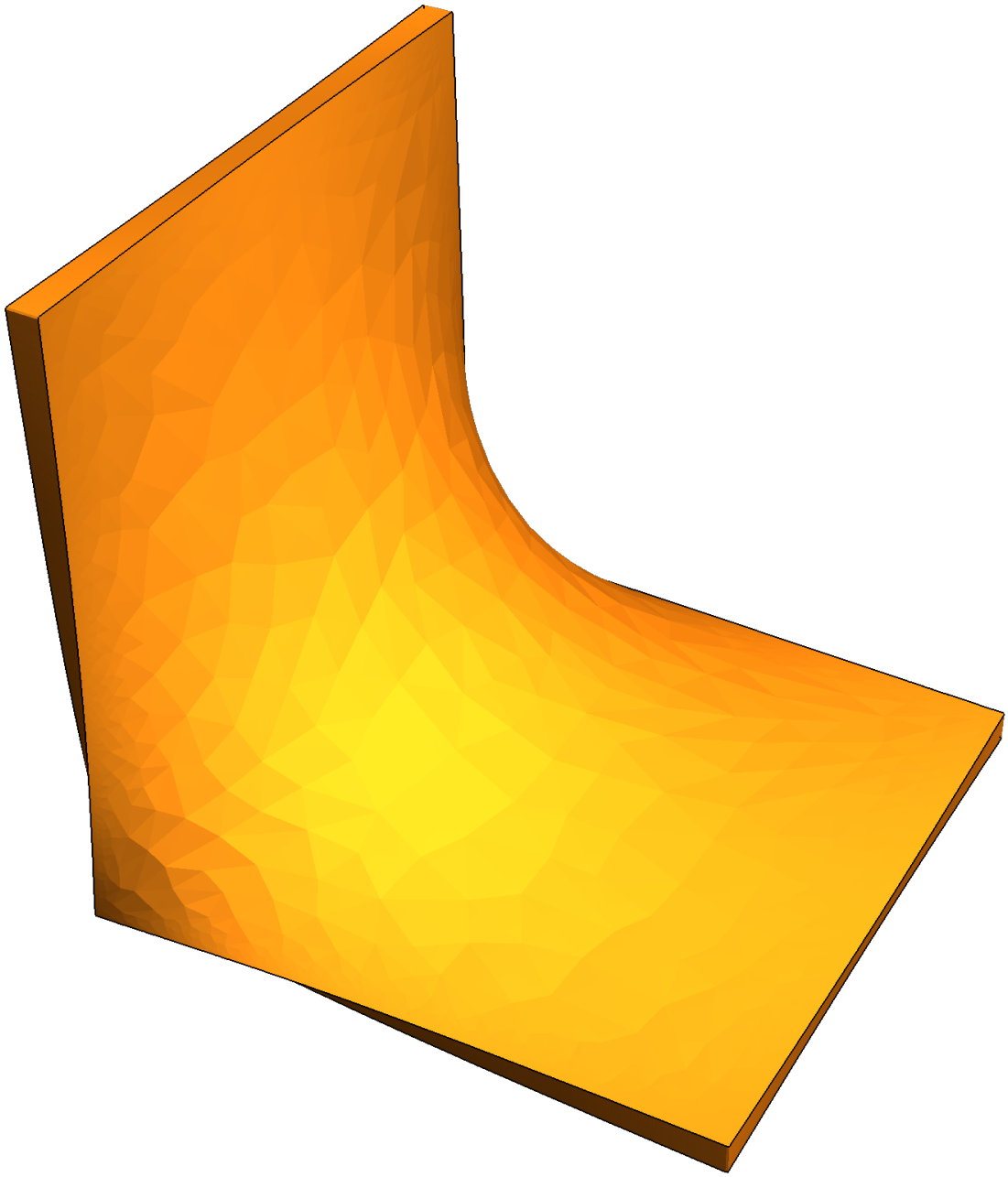

Figure 2: The singular surface in R_3 bounded by soccer gate loop. The Clebsch field is discontinuous at this surface with normal derivatives vanishing on both sides. Vorticity is continous and directed towards the local normal.

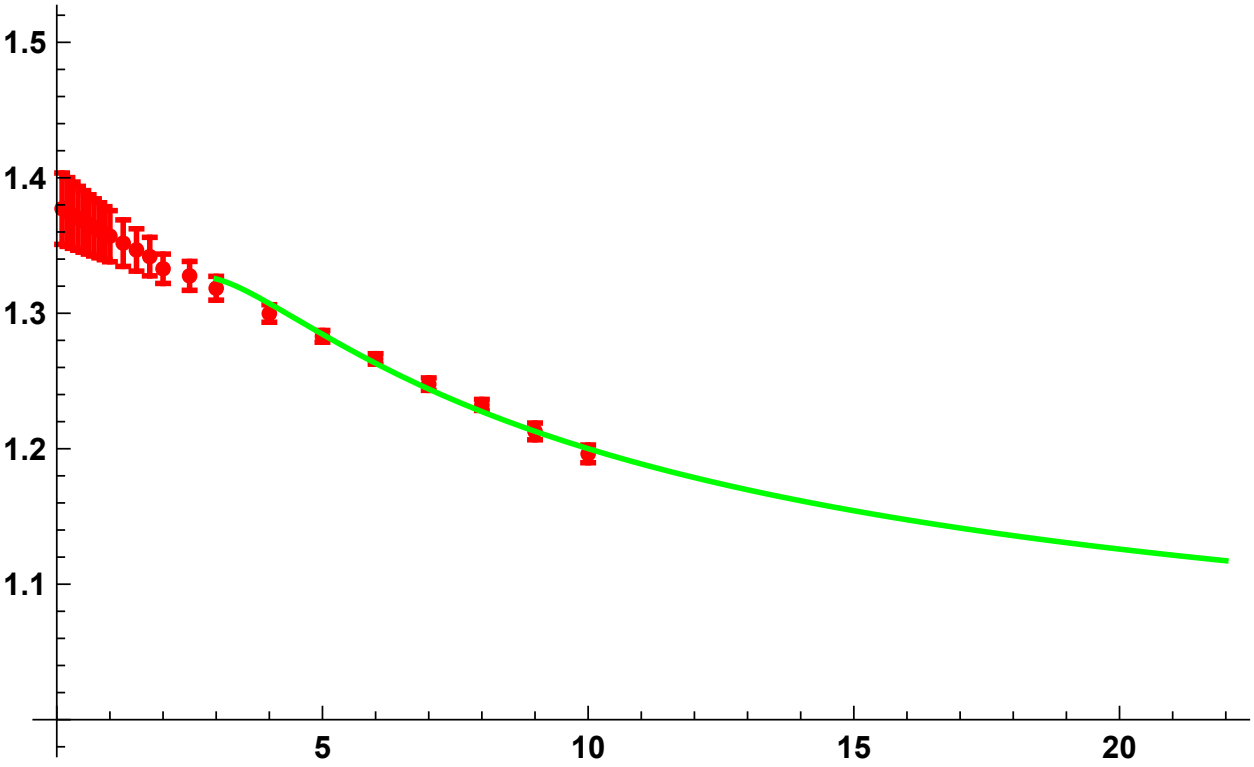

Figure 3: Here is the plot of effective index $2\alpha_{eff}(p)$ with the green line corresponding to our fit $2\alpha_{eff}(p) = 1 + 0.92\frac{\log p}{p}$. The data with error bars (red) was taken from [12].

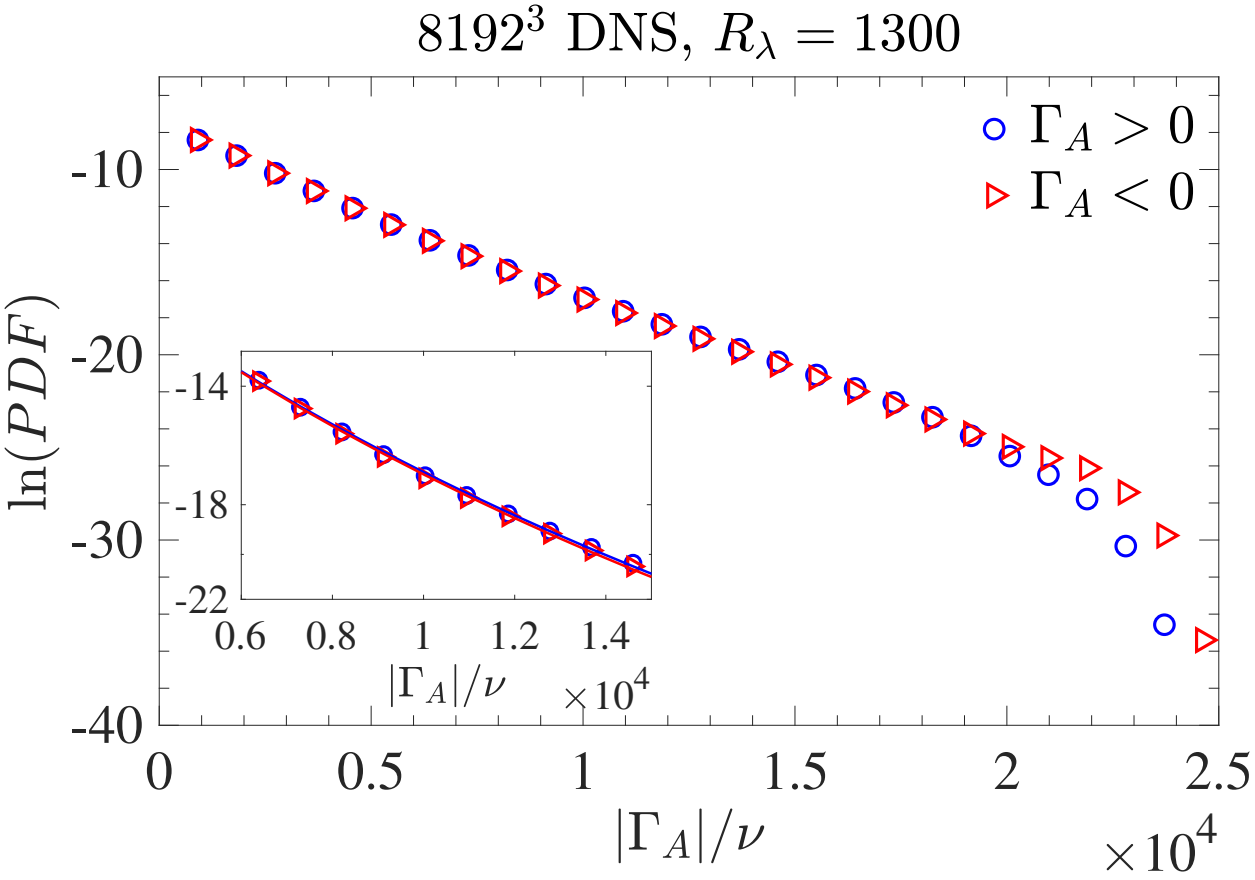

Figure 4: The circulation PDF as measured in [12]. The tails are perfectly symmetric and exponential down to PDF $\sim 10^{-10}$ within statistical errors. The linear fit is shown on a zoomed part.